Int J Adv Manuf Technol (2016) 86:2885–2894
DOI 10.1007/s00170-016-8394-x

ORIGINAL ARTICLE

Precision dicing of hard materials with abrasive blade

L. A. O. Araujo[1] · C. R. Foschini[2] · R. G. Jasinevícius[1] · C. A. Fortulan[1]

Received: 3 August 2015 / Accepted: 15 January 2016 / Published online: 4 February 2016

Abstract The present work shows the experiments on dicing of high alumina substrates using abrasive blades. The technology used by modern electronic components is based on narrow and thin ceramic and single crystal substrates. One of the techniques used to obtain these products is to dice a larger substrate using an abrasive blade to generate low damages and high productivity called dicing process. Samples with high alumina (99.8 %) were diced with diamond abrasive blades in a creep feed process. The process parameters were changed as cuts 1 to 3 mm deep were made. The feed speed varied from 1 to 19 mm/s and the blade rotation varied from 10,000 to 30,000 rpm. The blade wearing as well as the linearity and the quality of dicing were analyzed. Higher blade rotation increases the blade stiffness and on these experiments a more stable cutting process was achieved at 30,000 rpm. The removal material mechanism was also explored comparing the chipping between silicon and the high alumina specimens.

Keywords Precision dicing · Dicing saw · Dicing machine · Abrasive cutting process

✉ L. A. O. Araujo
luis.araujo@usp.br

[1] Mechanical Engineering Department, Universidade de São Paulo, Av. Trabalhador Saocarlense 400, 13566-590 Sao Carlos, SP, Brazil

[2] Faculdade de Engenharia de Bauru, Mechanical Engineering Department, Universidade Estadual Paulista, Av. Eng. Luiz Edmundo C. Coube, 14-01, 17033-360 Bauru, SP, Brazil

1 Introduction

In the last four decades, the use of silicon in the microelectronic industry has been the motivation for the development of the precision grinding and dicing processes in fragile materials. The evolution of the dicing technology opens the possibility to other applications and promotes the improvement and the development of many other products. Today, precision dicing is characterized mainly for its high productivity and the quality associated to increasingly smaller sizes and tolerances of the cut parts [1, 2]. This process is done in precision dicing machines. Unlike the cut-offs machines, the precision dicing machines offer higher precision and sophistication with respect to alignment of cutting on the part, types of cutting blades, repeatability, automation, and performance.

There are three types of precision dicing machines, according to its cutting element:

- Dicing saw—characterized by the use of abrasive blades as the cutting element. It comprises of a high rotation bearing, in general aerostatic or ceramic bearings. It has an accuracy as small as 1 μm and works with cutting speeds (feed speed) varying from 0.1 to 600 mm/s depending on the material to be diced. The blade could reach up to 60,000 rpm and a blade with a diameter of ~51 mm would reach a peripheral speed of up to 160 m/s. Basically, the quality of kerf depends on the combination of the material on work and parameters from process, as cooling system, feed speed, type of blade, peripheral speed, etc. [3].
- Laser saw—it uses a laser beam as cutting element. It can be YAG or CO_2, in different wave length and power. Although its application is restricted to thin films, kerfs' width is around 15 μm and very precise. It is possible to make different geometries of cut, not just straight. It is a

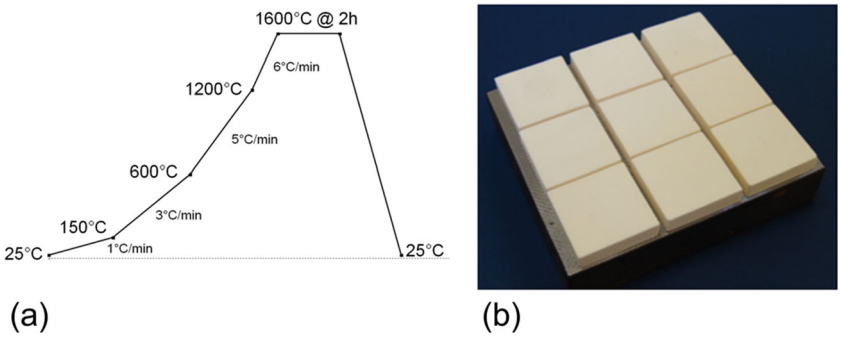

Fig. 1 **a** Firing profile for the sintering of Al_2O_3 tiles in air. **b** Arrangement of fired tiles mounted on a metal base in preparation for the dicing process

dry process, and the quality of kerf can be better than dicing saw, depending on the material on process [4].

- Water saw or jet saw is a cutting machine which uses a combination of water at high pressure and abrasive grains scattered in a fluid. In general, the quality of kerf is worse than the two previous and it is also a lower speed process than laser and dicing saw but with the best thermal heating characteristics. It can also make curvilinear [5].

Despite the flexibility in programming the cutting path, the laser saw and the water saw have the disadvantage of the limited thickness and quality of cutting. For these reasons, the dicing saw is the most widespread cutting process for fragile materials such as silicon, alumina, single crystals, and glass-ceramics among others.

The parts cut by a dicing saw have their geometry defined by the nature of the abrasive cut made. The defects generated during such processing have direct influence on the quality and performance of the final product, for example, microelectronic components made in silicon, quartz, etc. Defects from dicing process, such as macro or micro-cracks, chipping, deviations from linearity, and angled cuts, can have some influence in reading or information processing on the final product.

These modern products for the maintenance of integrity must be addressed with high rates of productivity, and on the operational limit, defects can be introduced and are dependent on material characteristics, abrasive grain size concentration on the blade, and the type of bonding matrix (resinoid, vitreous, or metallic), cut depth, peripherical speed of the blade, feed speed, contamination on the disc, cooling, chip removal rate, etc. [6, 7]. Some materials, when subjected to the cutting process, follow certain standards of cracking and chipping [6]. It is important to understand the influence of the process parameters and connect it to the damages introduced during dicing process. Based on this, it is possible to prevent mistakes, reduce cost, and increase productivity. Silicon is an example of the importance of this study. It is the most used material in electronic components due to its mechanical and electronic properties. An electronic component based on silicon takes many operations to reach the final configuration, dicing it is one of the steps and must be under control, due cost and time.

Most scientific work in the area of precision dicing is focused on the use of an abrasive dicing saw to cut silicon substrates for the microelectronics industry. Because of this, little is known about the performance of precision dicing of other materials, as ceramics.

Given the growing application of the machining process of precision dicing on the fabrication of different products (such as ceramic sensors, including single and multilayer, piezoelectric sensor and others), it was considered important by the

Table 1 Specifications of the dicing blade used

Characteristics of dicing blade	
External diameter (D)	57.15 mm
Thickness (e)	0.254 ± 0.010 mm
Grain size	54 μm
Resin-bond	Designed for materials such as ceramics and crystalline materials

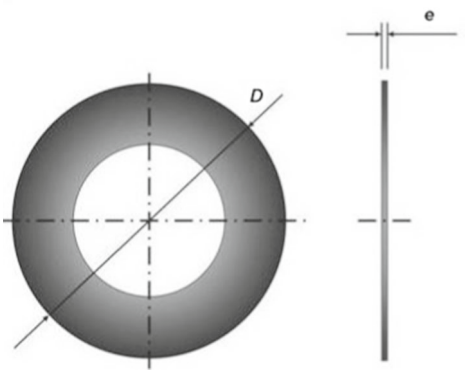

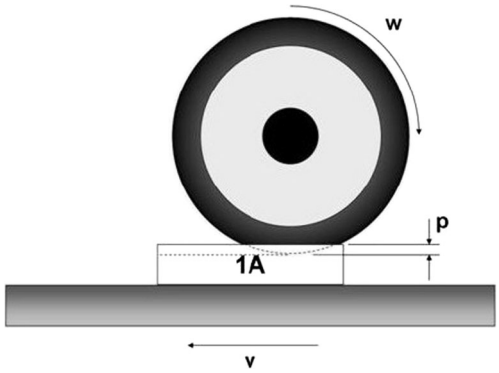

Fig. 2 Schematic of the cutting process

authors to study the performance of this tool on such materials, due several applications of ceramics in micro components, as implants or a micro heat transfer substrate. This paper reports on their investigation of the precision dicing on high alumina substrates, from the point of view of dicing performance (blade wear, feed speed, etc.) and surface finished (roughness of surface generated and chipping edge).

In addition, this study also reaches conclusions related with the material removal mechanism for hard materials, comparing silicon and alumina in very similar cutting conditions.

2 Experimental procedure

A methodology was developed for the study of high precision dicing on alumina test specimens. Fired alumina blocks were selected as test samples based on the commercial availability of the precursor powder, high degree of brittleness and hardness of the fired samples (expected around 1811 HV [8]), as well as for the low cost and easy of manufacture. The raw material properties and tile manufacturing process are well known which makes it a material of choice for the purpose of this work.

2.1 Raw material and processing

Test specimens alumina (Al_2O_3) were prepared from commercial powders 30 vol% alumina (Almatis Inc, A1000-SG, 99.8 %, average particle diameter of 0.4 μm, a surface area of 7.7 m^2/g, and a theoretical density (ρ_{th}) of 3.99 g/cm^3), 1 vol% of polyvinyl alcohol (PVA) (Vetec Química Fina Ltda—MW 22,000), 1 vol% of ammonium polyacrylate (Dispersal 130, Lubrizol), and 68 vol% of distillated water. Materials were introduced into a polyethylene jar (volume of 400 mL) containing 900 g of ceramic milling elements (regular alumina cylinders of ½") and mixed in a jar mill for 2 h followed of spray dried agglomeration.

The dried powder was uniaxialy pressed at 80 MPa followed by cold-isostatic pressing at 100 MPa for 0.5 min. The shape and dimensions of the as-pressed green test specimens were tiles of 40 × 40 × 10 mm. The dimensions after sintering in air at 1600 °C for 2 h were approximately 34 × 34 × 8.5 mm as shown in Fig. 1.

Table 2 Experimental parameters for high alumina specimen

Test specimen	Test (cut)	Speed rotation of the blade (*w*) (rpm)	Cutting depth (*p*) (mm)	Feed speed (*v*) (mm/s)
01	1A	30,000	1	1
	1B			3
	1C			5
	1D			7
	1E			9
	1 F			11
	1G			13
	1H			15
02	2A....2H		2	1.....15
03	3A....3H		3	1.....15
04	4A....4H	20,000	1	1.....15
05	5A....5H		2	1.....15
06	6A....6H		3	1.....15
07	7A....7H	10,000	1	1.....15
08	8A....8H		2	1.....15
09	9A....9H		3	1.....15
10	10I	10,000	3	17
10	10 J*			19

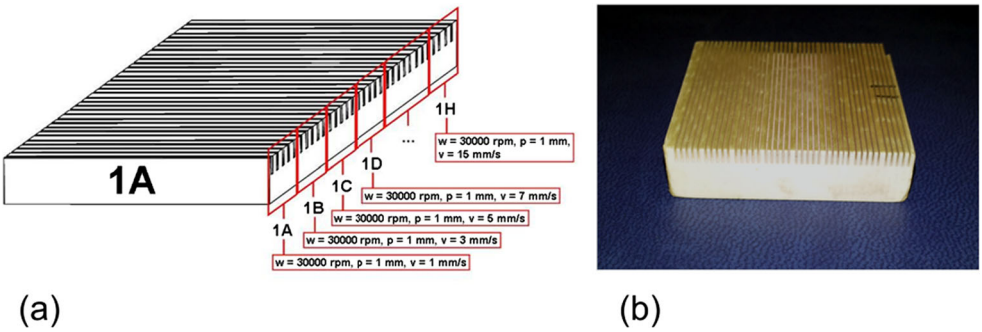

Fig. 3 Schematic of a diced tile and cutting parameters per section of the tile

2.2 Grinding of the test specimens

Two groups with nine pieces each were adhered on a tempered grinded steel block with 1 μm as the maximum parallelism deviation between its two faces, and which had one side with a groove pattern for adhesive dispersion (Fig. 1). The adhesive used was a thermo wax (Lakeside 70C, Buehler). The two faces of the (34 × 34 mm) alumina blocks were grinded flat to ensure dimensional homogeneity and planarity. The tiles were machined in a mill fitted with a water-cooled resin bonded diamond wheel with average grain size of 91 μm and concentration of 0.66 g/cm^3. The conditions for material removal were as follows: peripheral speed grinding wheel, 27 m/s; feed speed grinding wheel, 3 mm/min; depth, 0.05 mm per pass.

2.3 Dicing parameters

The dicing blade characteristics are given in Table 1.

In each test specimen, the following parameters were evaluated in a group of five cuts: blade rotation (w); cut depth (p); feed speed (v) (Fig. 2).

Each group of cuts was named by a number and a letter. The specimens and respective cutting groups were listed in Table 2. Each group of cuts has different composition of parameters. The number indicates the specimen and the letter the position of the sequence of cutting groups. Specimen 1 is detailed as example. Specimens 2 to 9 are summarized in the table. The first group, 1A, was also pointed in the front face of the sample, to index sequence and represented on Fig. 3a, b is specimen 8A after cut (w = 10.000 rpm, p = 2 mm, v = 1 … 15 mm/s).

The specimen 10 has just two groups of cuts, I and J. Those explore the results of cutting in potential worst condition of work for the blade: adopting depth of 3 mm, speed rotation of the blade in 10.000 rpm, and feed speed higher than 15 mm/s. Group J was marked with an asterisk indicating a failure in the cutting. It will be presented on the results section.

The dicing machine used was a DAD3350, DISCO Corporation; this model has resolution of 0.1 μm and alignment between axis (X, Y, and Z) less than 1.3 μm. Feed speed is from 0.01 to 600 mm/s and maximum spindle speed of 60.000 rpm with a blade of 2 in.

Characteristics related with the blade and the results of the quality of cuts were monitored: blade wearing (mm) was checked after each cutting group, by a laser sensor equipped in the dicing machine. Cutting power, expressed by the electric current of the motor (ampere) during cutting, was also monitored by the dicing machine. Surface roughness (Ra and Rrms) and the chipping in the edge of the cut were analyzed by topographic profile by a laser profilometer.

2.4 Silicon (111) wafer sample

A silicon wafer sample was also diced with similar equipment and cutting conditions: similar blade, rotation of 10,000 and 30,

Table 3 Experimental parameters for silicon wafer (111)

Test specimen	Test (cut)	Speed rotation of the blade (w) (rpm)	Cutting depth (p) (mm)	Feed speed (v) (mm/s)
Silicon wafer (111)	$11\overline{2}$	30,000	0.1	1
				5
			0.35	1
				5
		10,000	0.1	1
				5
			0.35	1
				5

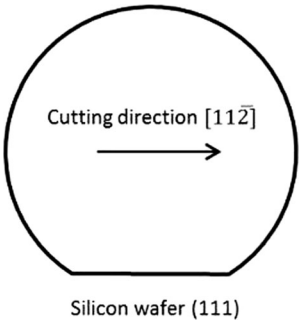

Fig. 4 The direction of cutting adopted for silicon wafer (111)

000 rpm, and feed speed of 1 and 5 mm/s. Cutting depth was restricted by the wafer thickness (0.5 mm). It applied cutting depth of 0.1 and 0.35 mm. Table 3 summarizes this combination of experimental cutting parameters for silicon (111).

The direction of cutting adopted was $11\bar{2}$ (Test cut), according with that indicated in Fig. 4. The idea of this experiment is a qualitative and quantitative comparison between those two materials and the removal mechanism, mainly because silicon is applied in various studies of cutting, and it is a clear reference for comparison.

The qualitative comparison is an image analysis of the quality of kerf and chipping at the edge. The quantitative comparison is a measurement of the chipping, as described in Fig. 5. The final dimensional of chipping will be an average of dimensions obtained in a length cut of 30 mm (for alumina and silicon). Cutting parameters will be the same except by the depth.

3 Results and discussion

The results were divided into two main groups for analysis: the characterization of the specimens and the performance of the dicing process.

Table 4 Properties of the alumina samples after sintering

Linear shrinkage (%)	Apparent porosity (%)	Total porosity (%)	Total density/theoretical density (%)
15.12 ± 0.14	0.54 ± 0.05	3.88	96.12 ± 0.017

3.1 Test specimen characteristics.

On Table 4, the average linear shrinkage, apparent and total porosity, and the densification rate of the specimens are presented.

The porosity around 4 % is relatively high and can be attributed to the low compaction pressure (100 MPa) and relatively low sintering temperature (1600 °C, 2 h) for an alumina 99.8 %. On the images obtained by scanning electron microscopy on the sample surface after dicing, this porosity should be considered.

3.2 Dicing performance—image analysis

Dicing performance is based on the capacity to remove material with a diamond blade (a mix of diamond grains and resin bond). If the material to be cut has hardness almost as diamond, the cutting parameters must be analyzed to keep a good level of quality, producing cuts geometrically acceptable and without damages (chipping on the edges).

From the experimental conditions, the test specimens 1 and 9 were selected for analysis. Group 1A took more time for cutting comparing with 9H, due to very low feed speed. Comparing both, speed rotation was higher and depth smaller in group 1A, and those are also positive conditions to obtain reduced chipping. The result from groups 1A and 9H can be analyzed on Fig. 6.

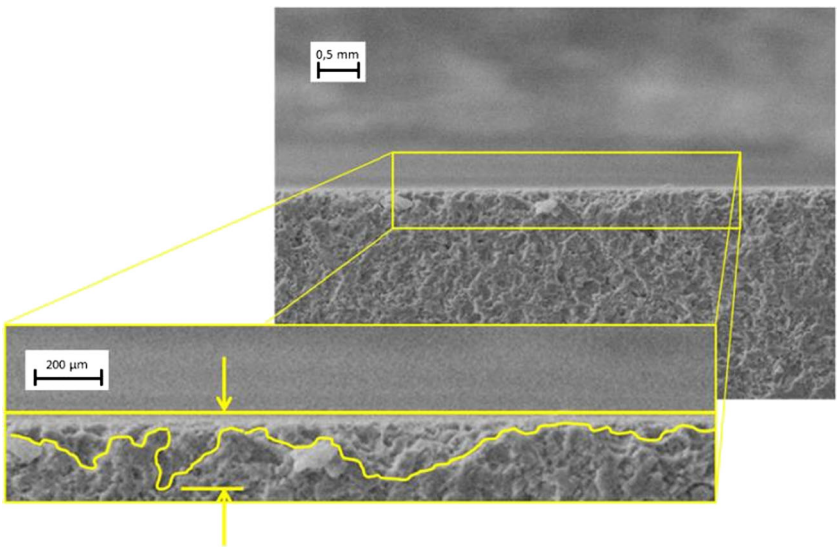

Fig. 5 Measuring chipping procedure

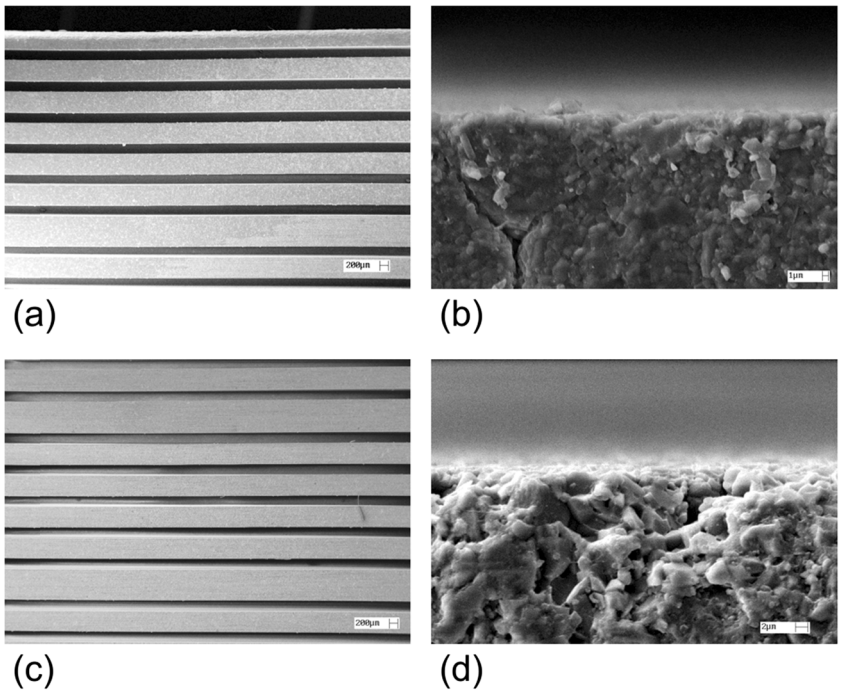

Fig. 6 Test specimen **a** after the surface grinding; **b** profile of the cross section roughness; **c** channel generated on the surface after the dicing process with a depth of 0.3 mm; **d** profile of roughness measured on the channel

Figure 4 shows those two sets of specimens after successive cuts. The 1A cutting group is presented in Fig. 6a and detailed cutting edge on Fig. 6b, similar for group 9H, Fig. 6c, d. From these images, 1A is less aggressive and the integrity of the edge was preserved. But in 9H, major fractures in the intergranular shape could be seem.

Distance between cuts is more regular on 1A than 9H, resulted from blade flexing. This fact can be explained analytically by a very simple geometric relation and by Kim et al. [6]. Misalignments during cuts can be generated by lateral forces, but it can just be generated if an external force is applied in the lateral face of the blade or if it has a very small flexion deformation. The lateral force would be a result of the angle (β) generated in the flexion. In this case, the cutting force has direct influence. As much as it is high, loose linearity can be more frequent. Figure 7 is a schematic of the situation.

Cutting force described by Kim et al. [6]:

$$\mathrm{Fr} = \sqrt{\mathrm{Ft}^2 + \mathrm{Fn}^2}$$

Where

$$\mathrm{Ft} = k \,.\, e \,.\, \left(\frac{v}{w} \,.\, a\right)^{\alpha}$$

And

$$\mathrm{Fn} = \lambda \,.\, \mathrm{Ft}$$

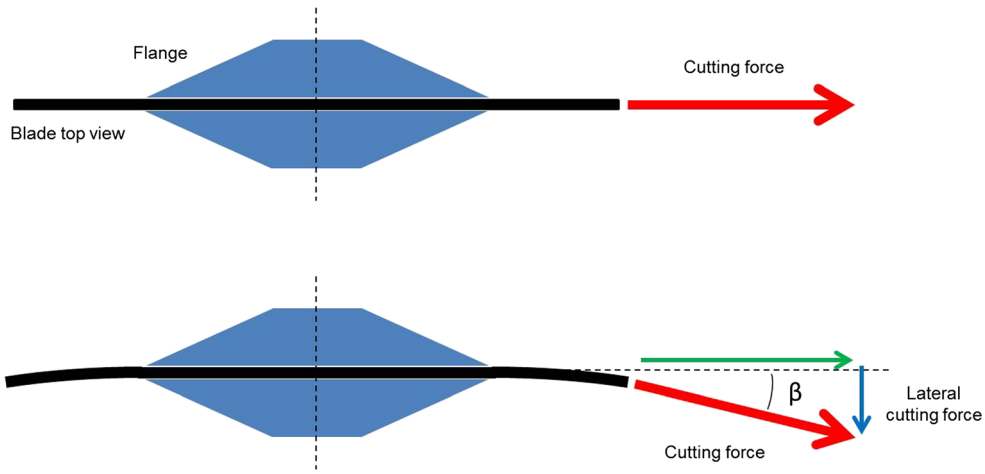

Fig. 7 Schematic description of the loss linearity of the cut due lateral force

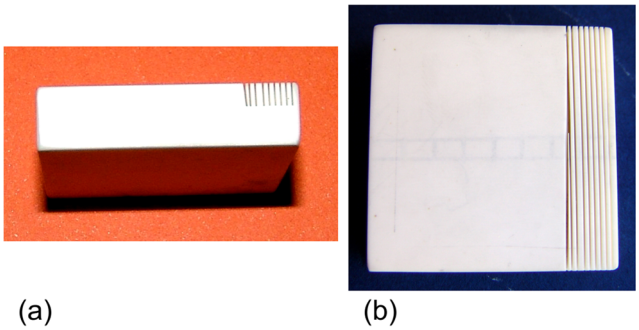

Fig. 8 Side view and top view of the blade entry in the specimen

Where λ is a constant, k is constant 2.19×10^6, e is the blade thickness, v is feed speed, w is rotation speed of the blade, and α is constant 1.41.

Comparing both conditions, it is possible to affirm that lateral force is bigger on situation 9H than 1A, and this explains the geometrical distortion of the cut on respective cutting group.

Situations 10I and J are very aggressive for the blade stability, due to higher feed speed. The result was a complete breakage of the blade and a very visual misalignment in the cut (Fig. 8).

Panel a of Fig. 9 presents the profile of the cut 1A and in panel b the longitudinal profile of the cut 1A, close (1 μm) from the edge, where the roughness measured were Ra = 0.15 μm and Rrms = 0.23 μm.

In panel c of Fig. 9, the profile of the cutting on the specimen 9H is presented, and in panel d the longitudinal profile of the cut 9H, near (1 μm) the edge, where the roughness measured were Ra = 0.42 μm and Rrms = 0.64 μm.

These profile measurements are strong evidences of the loss of integrity of the cutting process observed on the scanning electron microscopy (Fig. 6).

In another hand, Fig. 10 presents the images of a grinded test specimen before and after the cutting process. Panel a of Fig. 10 shows the three-dimensional image of the grinded surface before cutting and in panel b the profile of the cross section of this surface is presented, where the measured roughness was Ra = 0.233 μm and Rrms = 0.355 μm. Panel c of Fig. 10 shows the three-dimensional image of the surface with the channel generated after cutting with a programmed depth of 0.3 mm, feed speed of 1 m/s, and rotation of 30,000 rpm. In the channel valley, the measured roughness were Ra = 0.180 μm and Rrms = 0.290 μm. These measurements show that cutting process could improve the surface finishing even if it has high roughness surface.

3.3 Blade performance

The specification of the blade is important to reach a good level of quality for the cut. As described before, the cutting performance is based on the capacity of removed material with a diamond blade made by a mix of diamond grains and resin bond. The mechanism to remove material uses very small pockets to collect and move cut material from the front face of the blade. It is named "chip pockets." In these

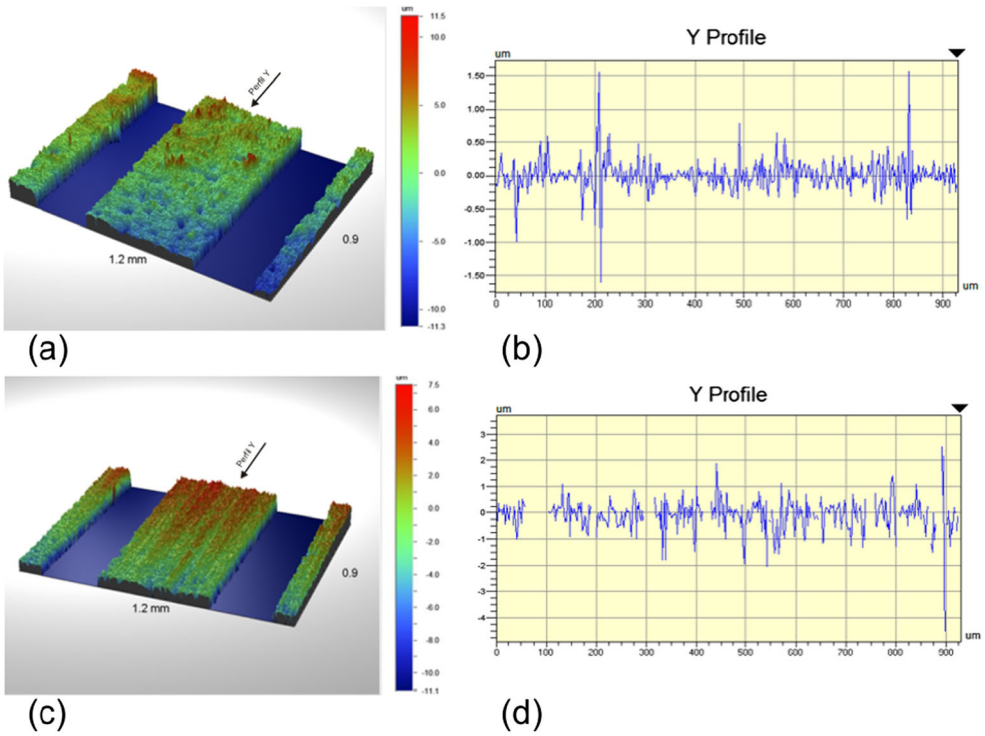

Fig. 9 Profiles of the roughness measurements on samples 1A (**a**, **b**) and 9H (**c**, **d**)

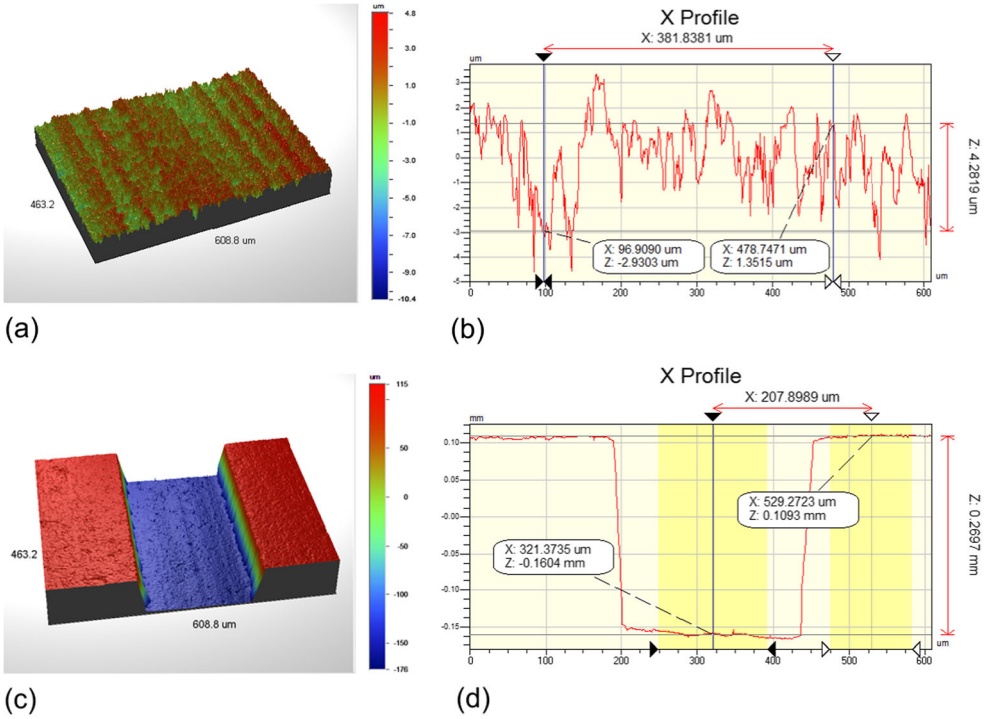

Fig. 10 Test specimen **a** after the surface grinding; **b** profile of the cross section roughness; **c** channel generated on the surface after the dicing process with a depth of 0.3 mm; **d** profile of roughness measured on the channel

experiments, it adopted a new blade (with the same specification) in each specimen.

After each cutting group, blade wearing was measured as a function of the feed speed and the results are shown on Figs. 11, 12, and 13. The blade wearing measured is high on low feed rates (below 4 mm/s) for all rotation speeds and depths analyzed. It could be related to the absence of the chip pockets, which are generated during the pre-cutting process. Generally, it suggested a dressing blade procedure before cutting, to create pockets along the blade.

As it was expected, the cutting forces, related to the power measured on the spindle, increased as the depth increased. The value of ampere was obtained during cutting. It also could be observed that the feed speed exerts small influence on the power over the spindle.

Combining the average wearing of three cutting depths (specimens from 1 to 3, 4 to 6, and 7 to 9) on each rotation speed of the abrasive blade, the performance curve was presented in Fig. 14.

According with the diagram for Fig. 14, generally, blade wearing happens in smaller rotation speed of the blade, 10,000 rpm as example. Feed speed between 7 and 13 mm/s has reduced blade wearing. However, if we compare with the microstructures on Fig. 6, the better cutting quality was observed at 30,000 rpm, for this type of material. Although the wearing is something that must be controlled in an abrasive process, in this case, it is necessary to reach a good level of quality.

3.4 Material removal mechanism—comparing silicon and high alumina

A wafer of silicon was submitted of similar cutting conditions as described before. The qualitative analysis indicates different chipping appearance between the two materials, as indicated in Fig. 15a, b. The morphological differences between ceramics and a single crystal reflect directly in the material removal mechanism.

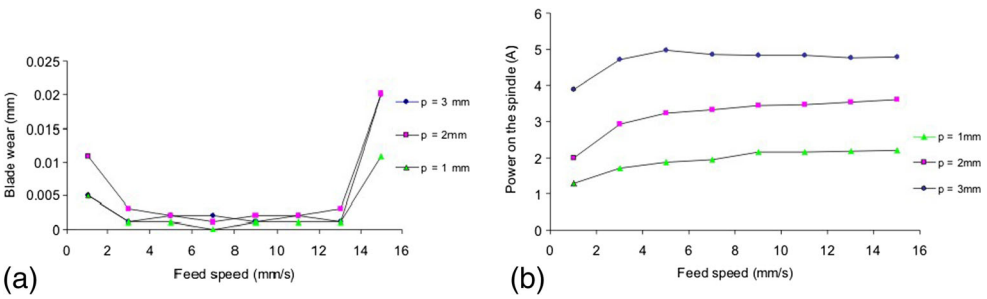

Fig. 11 Blade wearing and power on the spindle measured as a function of the feed speed for a rotation of 10,000 rpm

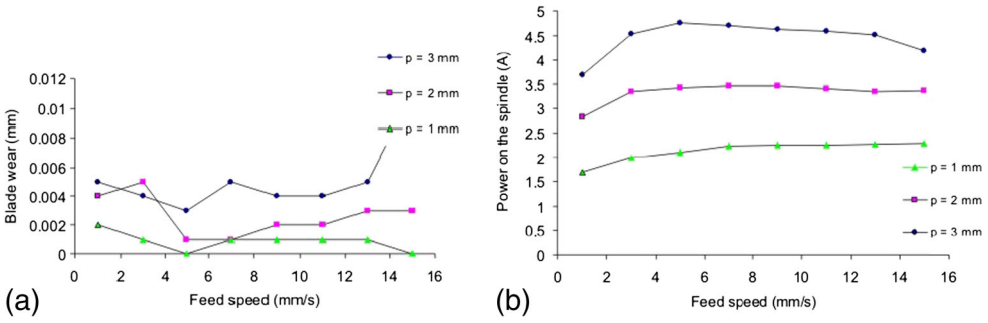

Fig. 12 Blade wearing and power on the spindle measured as a function of the feed speed for a rotation of 20,000 rpm

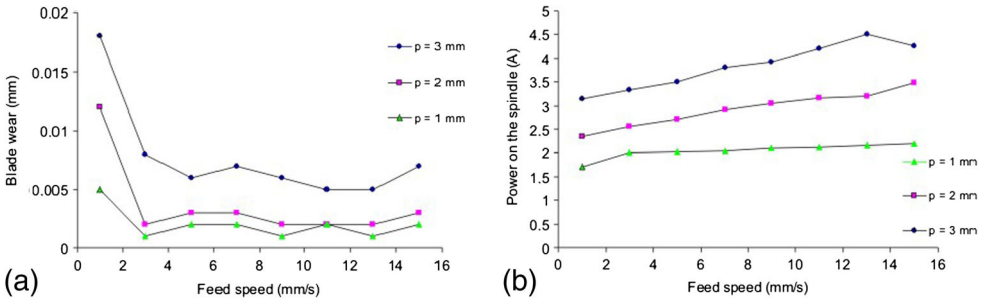

Fig. 13 Blade wearing and power on the spindle measured as a function of the feed speed for a rotation of 30,000 rpm

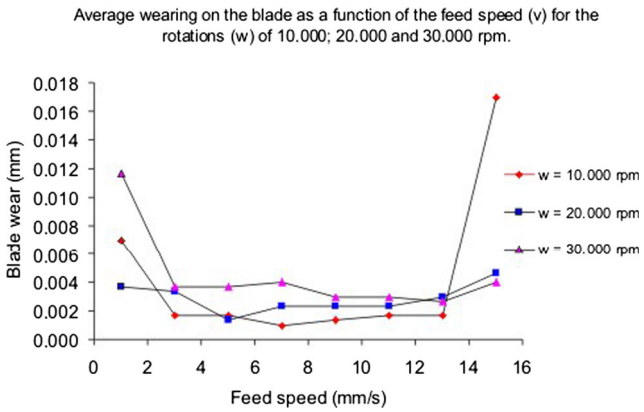

Fig. 14 Average wearing on the blades as a function of the feed speed for the rotations of 10,000, 20,000, and 30,000 rpm

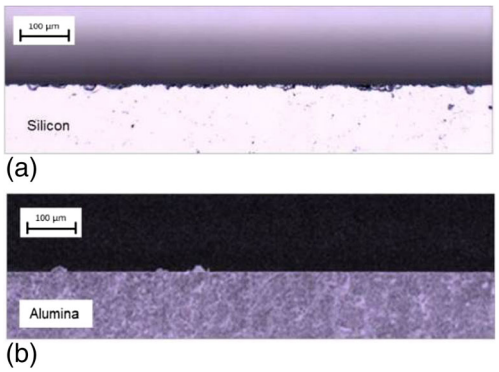

Fig. 15 Chipping appearance between **a** silicon (111) diced with $w = 30{,}000$ rpm, $p = 0.35$ mm, $v = 1$ m/s, and **b** high alumina, diced with $w = 30{,}000$ rpm, $p = 1$ mm, $v = 1$ mm/s

The material removing mechanism in a hard material, as silicon, follows three steps: rubbing, plastic deformation, and cracking [6]. In the case of a ceramic, the same mechanism occurs, but based on the grain level. In a critical situation of cutting, an entire grain or group of grains can be removed.

The quantitative analysis points a larger chipping in the silicon than in the alumina specimens. The dimension of chipping (average) is presented in Table 5. Except by the cutting depth, chipping tends to be smaller for high alumina. It is clear that the microstructure of the material under cutting process impacts directly in the dimension of the chipping.

4 Conclusion

The aggressiveness of the cutting process, which is higher p and v parameters, can cause damage to the quality of cutting and to the integrity of the diced substrate. It had already been observed, before the loss of linearity, damages in the cutting edge of the substrates.

According with Figs. 11a, 12a, and 13a, in the case of high alumina, blade wear increase in higher speed rotation and cutting depth. The blade wear also increase in feed speed lower than 5 mm/s and higher than 13 mm/s.

According with Figs. 11b, 12b, and 13b, the power consumption of the spindle increases with the cutting depth and reduces in higher spindle rotation. Feed speed has a small influence in the power consumption. This

Table 5 The dimension of chipping in silicon (111) and high alumina, according with speed rotation, cutting depth, and feed speed

Speed rotation of the blade (*w*) (rpm)	Cutting depth (*p*) (mm)	Feed speed (*v*) (mm/s)	Chipping silicon (μm)	Chipping alumina (μm)
30,000	0.1	1	64.3	–
		5	88.7	–
	0.35	1	90.2	–
		5	88.4	–
	1	1	–	18.0
		5	–	18.6
	3	1	–	18,7
		5	–	18.8
10,000	0.1	1	63.3	–
		5	96.7	–
	0.35	1	94.9	–
		5	102.5	–
	1	1	–	20.1
		5	–	20.9
	3	1	–	21.6
		5	–	22.8

can be comprehended as an indirect measurement of cutting forces.

The relation between feed speed, speed rotation, and size of chipping can be considered similar for both materials (silicon (111) and high alumina). But, different from a single crystal, the high alumina chipping occurs in the grain level, where it is possible to find intergranular and transgranular mechanism of removal. The grain size of the high alumina (in the case of this experiment, alumina had average particle diameter of 0.4 μm) applied for this experiment can be considered the main contribution for the reduced chipping.

The chipping size comparison between the two materials can indicate smaller damage in the high alumina than silicon single crystal substrate, except by the mechanism of removal. Basically, the single crystal process removal is based on elastic, plastic, and fracture, different from alumina that is essentially inter- and transgranular.

References

1. Mizuno M, Iyama T, Zhang B (2008) Analysis of the sawing process with abrasive circular saw blades. J Manuf Sci Eng 130:011012-1–011012-15
2. Efrat U (1993) Optimizing the wafer dicing process. Fifteenth IEEE/CHMT Int. Electronics Manufacturing Technology Symposium, pp. 245–253
3. Lin J, Cheng M (2014) Investigation of chipping and wear of silicon wafer dicing. J Manuf Process 16(3):373–378
4. Cheung A T (2005) Dicing advanced materials for microelectronics. Advanced packaging materials: processes, properties and interfaces. International Symposium, pp. 149–152
5. Perrotet D, Durant P, Richerzhagen B (2006) Water-jet-guided laser technology a damage free dicing solution. Adv Packaging 15(6):24–26
6. Kim S, Lee E, Kim N, Jeong H (2007) Machining characteristics on the ultra-precision dicing of silicon wafer. Int J of Adv Man Tech 33: p662–p667
7. Luo SY, Wang ZW (2008) Studies of chipping mechanisms for dicing silicon wafer. Int J of Adv Manuf Technol 35:p1206–p1218
8. Curkovic L, Rede V, Grilec K, Mulabidic A (2007) Hardness and fracture toughness of alumina ceramics. Conference of Materials, Processes, Friction and Wear.